Springer

Journal of Mechanical Science and Technology 23 (2009) 229~236

Journal of
Mechanical
Science and
Technology

www.springerlink.com/content/1738-494x
DOI 10.1007/s12206-008-1105-2

Modeling of a hydraulic engine mount for active pneumatic engine vibration control using the extended Kalman filter †

Arjon Turnip, Keum-Shik Hong* and Seonghun Park

School of Mechanical Engineering, Pusan National University; San 30 Jangjeon-dong Gumjeong-gu, Busan, 609-735, Korea.

(Manuscript Received October 3, 2008; Revised November 4, 2008; Accepted November 11, 2008)

Abstract

The attenuation of engine vibration transmitted to a chassis has been a major focus in the automotive community for the increase of comfort for the driver and passengers. A hydro-mount system is designed to reduce the transmission of engine vibration to the chassis. It is also used for supporting the static load by an engine weight. In this paper, we present a modeling and parameter estimation of hydro-mount systems. Nonlinear model aspects are developed and used with experimental data to validate the model response characteristics. These parameters will be modeled as a variable vector and its value is estimated via linearized and extended Kalman filter. This approach can help engineers reduce design time by providing insight into the effects of various parameters within the hydro-mount. Based on the estimated parameters, the simulation result confirmed that the derived passive model describes the dynamic behavior of the hydro-mount system accurately.

Keywords: Hydraulic engine mount; Modeling; Parameter estimation; Extended Kalman filter

1. Introduction

An engine mount system has two basic functions: one is to support the weight of the engine and the other is to isolate engine vibrations. In vehicles, there are two significant vibration sources, vibrations from the engine and vibrations from the ground, which should be reduced to enhance the comfort of passengers. The engine vibrations typically contain frequencies in the range of 20-200 Hz with amplitudes generally less than 0.3 mm. On the other hand, the main part of chassis vibrations involves frequencies under 30 Hz with amplitudes greater than 0.3 mm [1-3]. In this paper, we focus on modeling and parameter estimation of a hydraulic mount (hydro-mount in short) system.

A hydro-mount system is naturally required to have a high dynamic stiffness to support the engine weight. However, it also should transmit as less vibration from the engine to the chassis as it can. To achieve this (i.e., vibration isolation), the engine mount system should also satisfy a low dynamic stiffness [3,4]. It is difficult to meet these conflicting demands with a passive engine mount system. To resolve this problem, an innovative hardware design as well as an efficient vibration control technique is needed. To reduce the time in designing a new engine mount for various types of cars, it is necessary to have a mathematical model to predict the behavior of the system before it is physically assembled. A good model is also a key element when designing an efficient control algorithm for the system. The closer the response of a mathematical model is to the real plant, the higher achievement of control performance.

Even though many researchers have investigated various hydro-mount systems, the analysis of their dynamics is not completely resolved yet. Lee and Singh [5] comparatively evaluated three competing models at low frequencies by assuming that the mount

† This paper was recommended for publication in revised form by Associate Editor Shuzhi Sam Ge

*Corresponding author. +82 51 510 2454, Fax.: +82 51 514 0685
E-mail address: kshong @pusan.ac.kr

system behaves as a linear time-invariant system. A lumped parameter linear model was analyzed in [6, 7]. In [8], mechanical models for a single-pumper were proposed and their dynamic stiffness equations were derived. The nonlinear characteristics of an engine mount on the system output frequency behaviors are analyzed in [9, 10]. Kim and Singh [1] have illustrated the applicability of such modeling techniques for limited frequency domains thereby introducing the limitation of the linear modeling techniques. In their work, they never considered the true decoupler switching mechanism. Upon the modeling technique in [1], a number of experiments were carried out for parameter identification [3, 6, 11-13]. A fluid-structure interaction finite element analysis method and a nonlinear finite element analysis method were used to determine the system parameters [14]. In improving the performance of an engine mount using an efficient and practical design procedure, all the necessary parameters were derived from frequency response measurements [15, 16]. According to the phenomena of fixed points and the constant value of dynamic stiffness in-phase at higher bands, a new parameter identification method was presented in [17-19].

There exist different principles of modeling and parameter estimation of an engine mount system. The one that will be presented and modeled in this paper is based upon real input and output experimental data. Nonlinear modeling aspects are developed and used with experimental data to validate the model response characteristics. A regular hydro-mount is modeled, and its nonlinear model is linearized, and its values are estimated via extended Kalman filter (EKF) [20-23]. The objective is to obtain the optimum parameters for the hydro-mount model. The purpose is to show that the modeling technique is satisfactory and can serve as a control model for the hydro-mount system. It is important that the developed model is highly close to the reality, because input and output experimental data that can be used to verify the hydro-mount system are given. Related to this work, we have not found any published paper yet on constructing an engine mount model that uses extended Kalman filter to estimate the parameters based on experimental data. The parameters of these models are usually determined by the manufacturer from first-principle numerical calculations, or by means of direct testing of the individual components. Based on the estimated parameters, the simulation results will confirm that the derived passive model accurately describes the dynamic behavior of the hydro-mount system.

The contributions of this paper are the following. First, a new mechanism of a hydro-mount system for active control is investigated. The proposed one is realized in the structure of a hydro-pneumatic engine mount that satisfies the conflicting criterion (i.e., to have both low and high dynamic stiffness). Therefore, an equivalent mass-spring-damper model with piston-cylinder structure is proposed, and a subsequent mathematical analysis on the model yields the transfer function that describes the passive dynamic characteristics of the hydro-mount system. Second, nonlinear model aspects are developed and used with experimental data to validate the model response characteristics. This finally results in a good model that has a high known correspondence to reality. However, the use of an extended Kalman filter as parameter estimator is simpler and cheaper instead of determining by the manufacturer from first-principle numerical calculations, or by means of direct testing of the individual components. It is felt that this contribution will help engineers in reducing mount design time by providing insight into the effects of various parameters within the engine mount.

The paper structure as follows. In Section 2, structure and a new dynamic modeling of the hydro-mount system are introduced. The mathematical model is established to obtain the transfer function of the hydro-mount system that can provide significant information for the design and control purposes. In Section 3, after an overview of extended Kalman filter, an application of the nonlinear parameter estimation algorithm based on experimental data is proposed. In Section 4, comparison of experiment and simulation result is provided. Conclusions are given in Section 5.

2. Modeling of a hydro-mount

A hydro-mount and its cross-section used in this research are depicted in Fig. 1(a) and Fig. 1(b), respectively. It has two mounting brackets: one for the engine and the other for the chassis. The hydro-mount consists of a primary rubber, four chambers with different volumes (the upper, working, air, and lower chambers), and the first and secondary orifices.

Briefly explaining where the hydro-mount is used, Fig. 2 shows a scheme for the active pneumatic engine vibration control considered in this paper (two regular rubber mounts and one hydro-mount will be used). The actuator in the lower right corner in Fig. 2 is a pneumatic system. The air pressure (control force) in the air chamber in Fig. 1(b) is generated by opening and closing a solenoid valve. Due to the difference between the ambient air pressure and the pressure in the vacuum tank, the air will flow in when the valve is open. Because of the decoupler, the forces generated in the air chamber can be transmitted to the engine or to the chassis. The detailed descriptions on how the control scheme in Fig. 2 works are left in other work. In this paper, the mathematical model of the hydro-mount in Fig. 1 will be the focus.

(a) An engine mount photo (Daeheung R&T Co., Ltd., Korea)

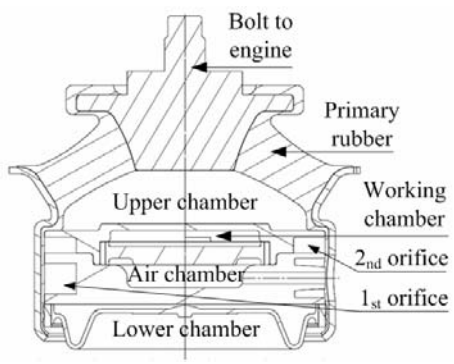

(b) A cross-section of the hydro-mount in (a)

Fig. 1. The typical hydraulic engine mount system considered in this paper.

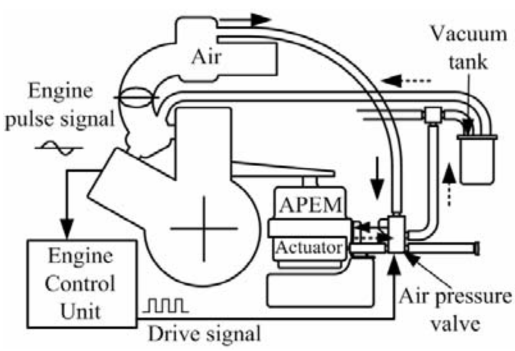

Fig. 2. Schematic of the proposed active pneumatic vibration control scheme using a hydraulic engine mount.

From Fig. 1(b), the functionalities of the hydro-mount are recapitulated in Fig. 3. Let $x(t)$ be the displacements of the engine, and let $F(t)$ and $F_T(t)$ be the engine excitation force and the transmitted force to the chassis, respectively. Let $P(t)$ and A_p be the pressure and the equivalent area of the upper chamber. The stiffness characteristics of the primary rubber is divided into two spring constants: the main spring constant k_r and the bulge spring constant k_p. Since the primary rubber supports the engine, the stiffness characteristics in the vertical deformation of the rubber at an equilibrium position is modeled as the main spring constant, whereas the variation of the stiffness characteristics of the primary rubber due to the pressure variation in the upper chamber is modeled as the bulge spring constant. Hence, the bulge spring constant becomes a function of the pressure in the upper chamber. The first orifice connects the upper chamber to the lower chamber and the second orifice connects the upper chamber to the working chamber, in which the orifices will equalize the pressures in individual chamber in the steady state. Also, to make the hydro-mount stiff in high frequency vibrations of the engine, a decoupler between the working chamber and the air chamber is used. The decoupler is made of a rubber or a fabric diaphragm. It can move freely in the passage connecting the two chambers. Since the mass of the decoupler is small, its dynamics are neglected in this paper.

Now, the hydraulic flows through the first and second orifices can be modeled as a second-order mass-spring-damper system as in Fig. 4. Let the cross-sectional areas of first and second orifices be A_1 and A_2, respectively. The amount of fluids flowing

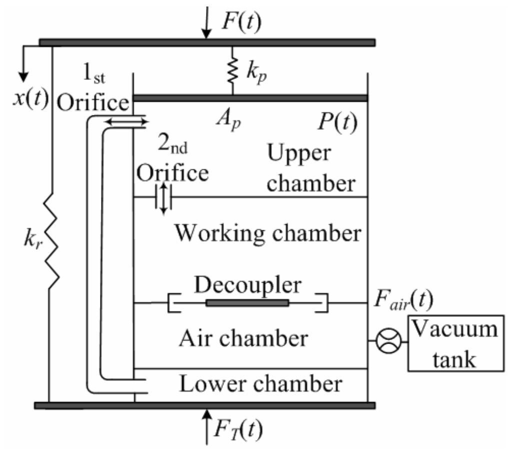

Fig. 3. A functionality diagram of the hydro-mount.

through two orifices are modeled as equivalent masses m_1 and m_2, respectively, with damping coefficients c_1 and c_2, respectively, and spring constants k_1 and k_2, respectively. Let $x_p(t)$, $x_1(t)$, and $x_2(t)$ be the displacements of the primary rubber, the equivalent mass in the first orifice, and the equivalent mass in the second orifice, respectively.

In Fig. 4, the force transmitted to the chassis, $F_T(t)$, is the system output, which is the sum of two forces that is to be controlled: an engine vibration force $k_r x(t)$ and a hydraulic force in the upper chamber $A_P P(t)$. Of course, $P(t)$ changes with flow changes in the first and second orifices as well as the change of $x(t)$. Now, the force transmitted to the chassis is expressed as follows,

$$F_T(t) = k_r x(t) + A_p P(t). \tag{1}$$

Since the fluid is assumed to be incompressible, the continuity equation holds as follows,

$$A_p x_p(t) = A_1 x_1(t) + A_2 x_2(t). \tag{2}$$

Note that the bulge spring constant is proportional to the pressure in the upper chamber. Also, the following equation at an equilibrium point is obtained,

$$-P(t) A_p = k_p \left(x_p(t) - x(t)\right). \tag{3}$$

The pressure variation in the upper chamber also makes the fluid to flow through the first and second orifices as shown below.

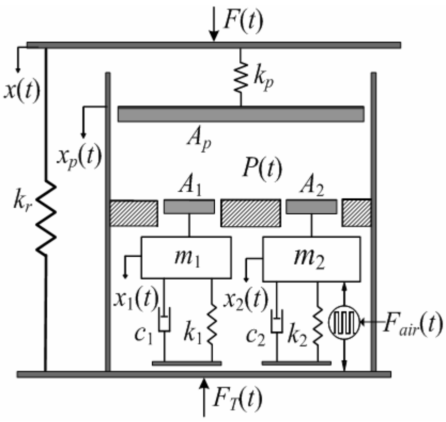

Fig. 4. The final schematic of the hydro-mount for modeling: fluid flows included.

$$m_1 \ddot{x}_1(t) + c_1 \dot{x}_1(t) + k_1 x_1(t) = A_1 P(t), \tag{4}$$

$$m_2 \ddot{x}_2(t) + c_2 \dot{x}_2(t) + k_2 x_2(t) + F_{air}(t) = A_2 P(t), \tag{5}$$

where $F_{air}(t)$ is the force exerted by the pneumatic actuator.

Taking the Laplace transform of Eqs. (1)-(5) and substituting Eqs. (2)-(5) into Eq. (1) yields

$$F_T(s) = A(s) X(s) - B(s) F_{air}(s), \tag{6}$$

where

$$A(s) = \frac{b_0 s^4 + b_1 s^3 + b_2 s^2 + b_3 s + b_4}{s^4 + a_1 s^3 + a_2 s^2 + a_3 s + a_4}, \tag{7}$$

$$B(s) = \frac{d_0 s^2 + d_1 s + d_2}{s^4 + a_1 s^3 + a_2 s^2 + a_3 s + a_4}, \tag{8}$$

and

$$\begin{aligned}
a_1 &= (1/m_1 m_2)(m_1 c_2 + m_2 c_1), \\
a_2 &= \left(1/m_1 m_2 A_p^2\right)\Big(m_1(k_2 A_p^2 + k_p A_2^2) \\
&\qquad + m_2(k_1 A_p^2 + k_p A_1^2) + c_1 c_2 A_p^2\Big), \\
a_3 &= 1/m_1 m_2 A_p^2 \Big(c_1(k_2 A_p^2 + k_p A_2^2) \\
&\qquad + c_2(k_1 A_p^2 + k_p A_1^2)\Big), \\
a_4 &= 1/m_1 m_2 A_p^2 \left(k_1 k_2 A_p^2 + k_p k_2 A_1^2 + k_p k_1 A_2^2\right), \\
b_0 &= k_r + k_p, \\
b_1 &= (1/m_1 m_2)\left((k_r + k_p)(m_1 c_2 + m_2 c_1)\right), \\
b_2 &= \left(1/m_1 m_2 A_p^2\right)\Big(A_p^p(k_r + k_p)(m_1 k_2 + m_2 k_1 + c_1 c_2) \\
&\qquad + k_r k_p(m_1 A_2^2 + m_2 A_1^2)\Big), \\
b_3 &= \left(1/m_1 m_2 A_p^2\right)\Big(A_p^2(k_r + k_p)(c_1 k_2 + c_2 k_1) \\
&\qquad + k_p k_r(c_1 A_2^2 + c_2 A_1^2)\Big), \\
b_4 &= \left(1/m_1 m_2 A_p^2\right)\Big(A_p^2 k_1 k_2(k_r + k_p) \\
&\qquad + k_p k_r(A_1^2 k_2 + A_2^2 k_1)\Big), \\
d_0 &= A_2 k_p / m_2 A_p, \quad d_1 = A_2 k_p c_1 / m_1 m_2 A_p, \\
d_2 &= A_2 k_p k_1 / m_1 m_2 A_p.
\end{aligned} \tag{9}$$

$A(s)$ and $B(s)$ are the transfer functions from the engine displacement to the transmitted force and from the control input (air force) to the transmitted force, respectively.

3. Parameter estimation: extended filter

In Eqs. (1)-(5), the coefficients k_r, A_p, A_1, A_2, m_1, and m_2 are known: k_r is obtained from experiment and all others are calculated using the geometry of the upper chamber, orifices and liquid properties. Unknown coefficients are k_p, c_1, c_2, k_1, and k_2. Since $x(t)$ and $F_T(t)$ are measured, $P(t)$ is calculated using Eq. (1). In this section, $x_1(t)$ and $x_2(t)$ in Eq. (2) and c_1, c_2, k_1, and k_2 in Eqs. (4)-(5) are estimated using the extended Kalman filter technique.

Eqs. (4) and (5) without actuation (i.e., $F_{air} = 0$) are now considered. Let

$$z_{1i}(t) = x_i(t)\,, \tag{10}$$

$$z_{2i}(t) = \dot{x}_i(t)\,, \tag{11}$$

$$z_{3i}(t) = c_i\,, \tag{12}$$

$$z_{4i}(t) = k_i\,, \tag{13}$$

where $i = 1, 2$. Hence,

$$\dot{z}_{1i}(t) = z_{2i}(t)\,, \tag{14}$$

$$\dot{z}_{2i}(t) = \ddot{x}_i(t) = (1/m_i)(-z_{1i}(t)z_{4i}(t) - z_{2i}(t)z_{3i}(t) + A_i P(t))\,, \tag{15}$$

$$\dot{z}_{3i}(t) = 0\,, \tag{16}$$

$$\dot{z}_{4i}(t) = 0\,. \tag{17}$$

Since $P(t)$ in Eq. (1) is calculated using the measured signals $x(t)$ and $F_T(t)$ which are assumed involves white Gaussian noise, the signal $A_i P(t)/m_i$ also involves white Gaussian noise $w_i(t)$ inherited from the measured signals. Then, Eqs. (4)-(5) can be rewritten as

$$\ddot{z}_{1i}(t) + \frac{1}{m_i} z_{1i}(t)z_{4i}(t) + \frac{1}{m_i} z_{2i}(t)z_{3i}(t) = A_i(F_T(t) - k_r x(t))/A_p m_i + w_i(t)\,. \tag{18}$$

In the state space form, Eq. (18) becomes

$$\begin{bmatrix} \dot{z}_{1i}(t) \\ \dot{z}_{2i}(t) \\ \dot{z}_{3i}(t) \\ \dot{z}_{4i}(t) \end{bmatrix} = \begin{bmatrix} z_{2i}(t) \\ -\dfrac{z_{1i}(t)z_{4i}(t)}{m_i} - \dfrac{z_{2i}(t)z_{3i}(t)}{m_i} \\ 0 \\ 0 \end{bmatrix} + \begin{bmatrix} 0 \\ 1 \\ 0 \\ 0 \end{bmatrix} w_i(t) + \begin{bmatrix} 0 \\ 1 \\ 0 \\ 0 \end{bmatrix} \frac{A_i(F_T(t) - k_r x(t))}{A_p m_i}\,. \tag{19}$$

The observation equation is

$$y_i(t) = z_{1i}(t) + v_i(t)\,, \tag{20}$$

where $v_i(t)$ is an observation noise which is assumed as a white Gaussian noise. The discrete nonlinear plant and linear observation equations for this model are

$$\begin{aligned} z_{1i}^k &= z_{1i}^{k-1} + T z_{2i}^{k-1}, \\ z_{2i}^k &= \left(T z_{4i}^{k-1}/m_i\right) z_{1i}^{k-1} + \left(1 - T z_{3i}^{k-1}/m_i\right) z_{2i}^{k-1} \\ &+ A_i T\left(F_T^{k-1} - k_r x^{k-1}\right)/A_p m_i + T w_i^{k-1}, \\ z_{3i}^k &= z_{3i}^{k-1}, \\ z_{4i}^k &= z_{4i}^{k-1}, \\ y_i^{k-1} &= z_{1i}^{k-1} + v_i^{k-1}, \end{aligned} \tag{21}$$

where T is the sampling time. By substituting the variables $x_i(t)$ in Eq. (10) to Eq. (2), the variable $x_p(t)$ in Eq. (2) can be estimated. Therefore, applying the value $x_p(t)$ to Eq. (3), the bulge spring constant k_p is finally calculated.

4. Experiments and simulations

To make an equilibrium state due to the engine weight, an 800 N force was applied as a preload to the experimental sample. In the experimental setup, only the engine generates vibrations (i.e., the chassis is stationary), and thus the measured values of $x(t)$ and $F_T(t)$ are the net engine displacement and the net transmitted force to the chassis, respectively. As discussed in the previous section, this vibration typically contains frequencies in the range of 20-200 Hz with amplitudes generally less than 0.3 mm.

To estimate parameters in Eq. (9) using the proposed parameter estimator algorithm Eq. (21), simulations of the hydro-mount using the same engine vibration data obtained from experiment were carried out. The used vibration is a typical idle speed of a 4-cylinder and 4-cycle in-line engine, whose excitation frequency is 25 Hz with amplitude of 0.1 mm.

The validity of the model derived in Eq. (6) was checked: the engine excitation and the actuator vibration independently contribute to the transmitted force. As a result, both the passive transfer function Eq. (7) and the active transfer function Eq. (8) were estimated separately. Based upon the real input $x(t)$ and the output $F_T(t)$, the variables $x_1(t)$ and $x_2(t)$ in Eq. (10) and the parameters c_1, c_2, k_1 and k_2 in Eq. (12) and Eq. (13), respectively, were estimated using the extended Kalman filter. The comparison between the simulated and the estimated variables of the first and the second orifices are depicted in Fig. 5 and Fig. 6, respectively, which show the closeness of both results. By substituting the estimated variables $x_1(t)$ and $x_2(t)$ in Eq. (10) to Eq. (2), the variable $x_p(t)$ is calculated and the result is shown in Fig. 7. Substitution of the calculated variable $x_p(t)$ to Eq. (3), the value of the bulge spring constant k_p is calculated approximately 19412 N/m whereas the remaining parameters were obtained from experimental and manufacturer.

Using the optimum parameters obtained via EKF (Fig. 5 and Fig. 6) for the proposed model, the hydro-mount behaviors are compared. Fig. 8 compares the output of the experimental data and the model of the hydro-mount one. The predicted dynamic stiffness and loss angle spectra of the hydro-mount system for low frequency are shown in Fig. 9. Although there are small differences in amplitude and time delay, the overall results in Fig. 8 and Fig. 9 show that the force transmitted to the chassis obtained from simulation match with that from measurements reasonably, which validate the proposed hydro-mount system models in Eq. (7).

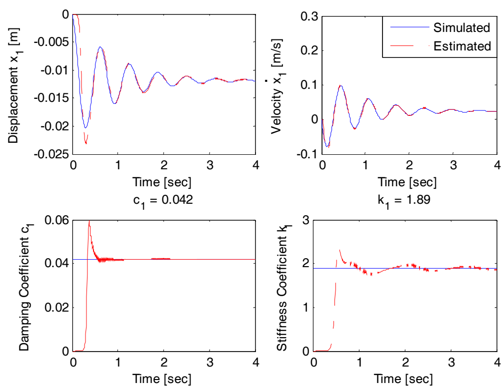

Fig. 5. Simulated and estimated variables of the first orifice.

5. Conclusions

In this paper, the modeling and parameter estimation of a hydro-mount system is presented. An equivalent mass-spring-damper model was proposed and mathematically analyzed to derive the transfer functions of passive dynamic characteristics of the hydro-mount. Nonlinear model aspects are developed and used with experimental data to validate the model

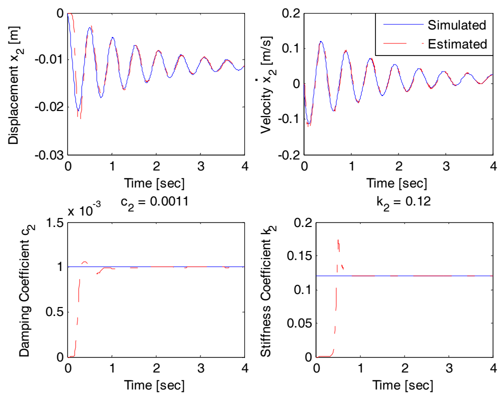

Fig. 6. Simulated and estimated variables of the second orifice.

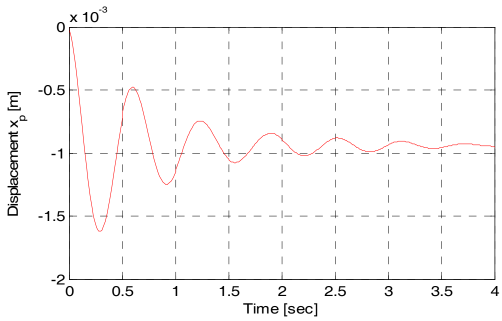

Fig. 7. Simulated primary rubber displacement.

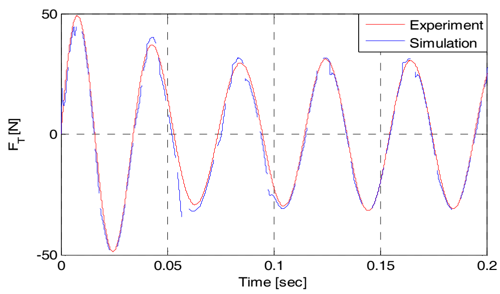

Fig. 8. Comparison of the force transmitted to the chassis by using experimental data and simulation.

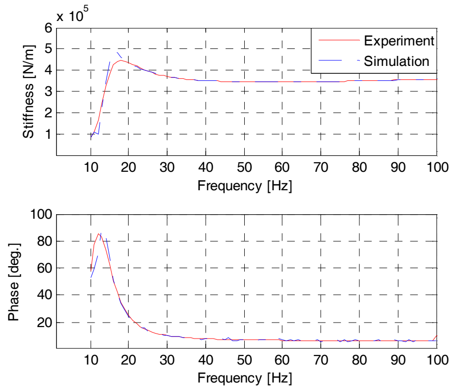

Fig. 9. Comparison of the dynamic stiffness by using experimental data and simulation.

response characteristics. Using the input-output experimental data and the obtained model, the parameters are estimated with extended Kalman filter. Based on estimated parameters, the simulation result confirmed that the derived passive model accurately describes the dynamic behavior of the hydro-mount system.

Acknowledgment

This work was supported for two years by Pusan National University Research Grant.

References

[1] G. Kim and R. Singh, A study of passive and adaptive hydraulic engine mount systems with emphasis on non-linear characteristics, *Journal of Sound and Vibration*, 179 (3) (1995) 427-453.

[2] Y. Yu, N. G. Naganathan and R. V. Dukkipati, A literature review of automotive vehicle engine mounting systems, *Mechanism and Machine Theory*, 36 (1) (2001) 123-142.

[3] Y. X. Zhang, J. W. Zhang, W.-B. Shangguan and Q. Sh. Feng, Modeling and parameter identification for a passive hydraulic mount, *International Journal of Automotive Technology*, 8 (2) (2007) 233-241.

[4] J. H. Lee and K.-J. Kim, An efficient technique for design of hydraulic engine mount via design variable-embedded damping modeling, *Journal of Vibration and Acoustics*, 127 (1) (2005) 93-99.

[5] J. H. Lee and R. Singh, Critical analysis of analogous mechanical models used to describe hydraulic engine mounts, *Journal of Sound and Vibration*, 311 (2008) 1457-1464.

[6] H. Adiguna, M. Tiwari, R. Singh, H. E. Tseng, and D. Hrovat, Transient response of a hydraulic engine mount, *Journal of Sound and Vibration*, 268 (2) (2008) 217-248.

[7] Y.-Q. Zhang and W.-B. Shangguan, A novel approach for lower frequency performance design of hydraulic engine mounts, *Computers & Structures*, 84 (8/9) (2006) 572-584.

[8] V. Nader, Double-notch single-pumper fluid mounts, *Journal of Sound and Vibration*, 285 (3) (2005) 697-710.

[9] Y. K. Ahn, J. D. Song, B. S. Yang, K. K Ahn, and S. Morishita, Optimal design of nonlinear hydraulic engine mount, *Journal of Mechanical Science and Technology*, 19 (3) (2005) 768-777.

[10] Z. K. Peng and Z. Q. Lang, The effects of nonlinearity on the output frequency response of a passive engine mount, *Journal of Sound and Vibration*, 318 (1/2) (2008) 313-328.

[11] S. He and R. Singh, Discontinuous compliance nonlinearities in the hydraulic engine mount, *Journal of Sound and Vibration*, 307 (3/5) (2007) 545-563.

[12] K. S. Hong, H. C. Sohn, and J. K. Hedrick, Modified skyhook control of semi-active suspensions: A new model, gain scheduling, and hardware-in-the-loop tuning, *ASME Transactions, Journal of Dynamic Systems, Measurement, and Control*, 124 (1) (2002) 158-167.

[13] W. S. Yoo, D. W. Park, M. S. Kim, and K. S. Hong, Optimum air pressure for an air-cell seat to enhance ride comfort, *International Journal of Automotive Technology,* 6 (3) (2005) 251-257.

[14] W.-B. Shangguan and Z.-H. Lu, Modelling of a hydraulic engine mount with fluid–structure interaction finite element analysis, *Journal of Sound and Vibration*, 275 (1/2) (2004) 193-221.

[15] S. Daley, J. Hätönen, and D. H. Owens, Active vibration isolation in a smart spring mount using a repetitive control approach, *Control Engineering Practice*, 14 (9) (2006) 991-997.

[16] D. H. Kim, K. S. Hong, and K. Yi, Driving load estimation with the use of an estimated turbine torque, *JSME International Journal, Series C,* 49 (1) (2006) 163-171.

[17] R. Fan and Z. Lu, Fixed points on the nonlinear dynamic properties of hydraulic engine mounts and parameter identification method: experiment and theory, *Journal of Sound and Vibration*, 305 (4/5)

(2007) 703-727.
[18] B. M. Seoudi, S.-H. Kim, H. H. Chun, and I. Lee, Numerical estimation of dynamic behaviour of viscoelastic elastomer specimen, *Journal of Mechanical Science and Technology*, 22 (6) (2008) 1140-1148.
[19] J. U. Chang, H. J. Ahn, and D. C. Han, Design parameter study of a permanent magnet biased magnetic actuator for improving stiffness and linearity, *Journal of Mechanical Science and Technology*, 21 (8) (2007) 1218-1225.
[20] J. Jung, S. Han, and K. Huh, Robust proportional-integral Kalman filter design using a convex optimization method, *Journal of Mechanical Science and Technology*, 22 (5) (2008) 879-886.
[21] J. Zhu, J. Park, K.-S. Lee, and M. Spiryagin, Robust extended Kalman filter of discrete-time Markovian jump nonlinear system under uncertain noise, *Journal of Mechanical Science and Technology*, 22 (6) (2008) 1132-1139.
[22] M. S. Grewal and A. P. Andrews, *Kalman Filtering: Theory and Practice using Matlab*, Second Ed. A Wiley-Interscience Publication, New York, (2001).
[23] F. V. D. Heijden, R. P. W. Duin, D.D. Ridder, and D. M. J. Tax, *Classification, Parameter Estimation and State Estimation*, John Wiley & Sons, Ltd, England, (2004).

Arjon Turnip received his B.S. and M.S. degrees in Engineering Physics from the Institute of Technology Bandung, Indonesia, in 1998 and 2003, respectively. He is currently a Ph.D. program student in the School of Mechanical Engineering, Pusan National University, Korea. His research areas are integrated vehicle control, adaptive control, and estimation theory.

Keum-Shik Hong received the B.S. degree in mechanical design and production engineering from Seoul National University in 1979, the M.S. degree in ME from Columbia University in 1987, and both the M.S. degree in applied mathematics and the Ph.D. degree in ME from the University of Illinois at Urbana-Champaign in 1991. He served as an Associate Editor for *Automatica* (2000-2006) and as an Editor for the *International Journal of Control, Automation, and Systems* (2003-2005). Dr. Hong received Fumio Harashima Mechatronics Award in 2003 and the Korean Government Presidential Award in 2007. Dr. Hong's research interests include nonlinear systems theory, adaptive control, distributed parameter system control, robotics, and vehicle controls.

Seonghun Park received his B.S. and M.S. degrees in mechanical engineering from KAIST in 1994 and 1996, respectively, and his Ph.D. degree from Columbia University in 2005. Dr. Park is currently a professor of mechanical engineering at Pusan National University, Korea. His research interests are in the areas of control, tribology, and biomechanics.